AIP | Applied Physics Letters

Enhanced stability in spin transfer nanopillars due to a Fe/Gd/Fe trilayer

Miguel Romera, Julie Grollier, Sophie Collin, Thibaut Devolder, Vincent Cros et al.

Citation: Appl. Phys. Lett. **103**, 122404 (2013); doi: 10.1063/1.4821510
View online: http://dx.doi.org/10.1063/1.4821510
View Table of Contents: http://apl.aip.org/resource/1/APPLAB/v103/i12
Published by the AIP Publishing LLC.

Enhanced stability in spin transfer nanopillars due to a Fe/Gd/Fe trilayer

Miguel Romera,[1] Julie Grollier,[2] Sophie Collin,[2] Thibaut Devolder,[3] Vincent Cros,[2] Manuel Muñoz,[4] and José L. Prieto[1]
[1]*Instituto de Sistemas Optoelectrónicos y Microtecnología (ISOM), Universidad Politécnica de Madrid, Avda. Complutense s/n, E-28040 Madrid, Spain*
[2]*Unité Mixte de Physique CNRS/Thales and Université Paris-Sud, 1 avenue A. Fresnel, 91767 Palaiseau, France*
[3]*Institut d'Electronique Fondamentale, Univ. Paris-Sud, 91405 Orsay, France and UMR 8622, CNRS, 91405 Orsay, France*
[4]*IMM-Instituto de Microelectrónica de Madrid (CNM-CSIC), Isaac Newton 8, PTM, E-28760 Tres Cantos, Madrid, Spain*

(Received 5 June 2013; accepted 2 September 2013; published online 18 September 2013)

A sharp antiferromagnetic boundary of Fe/Gd is found to affect notoriously the critical current for spin transfer torque (STT). Transport measurements performed on nano-patterned spin valves show that when a Fe/Gd/Fe is added as a top layer, the effect of spin transfer on the free layer is dramatically reduced. The critical current increases up to one order of magnitude at 10 K and five times at room temperature. We show that this increase cannot be fully explained by the macrospin approximation and we argue that it is due to a torque at the Gd/Fe interface that opposes the STT in the free layer. © *2013 AIP Publishing LLC*. [http://dx.doi.org/10.1063/1.4821510]

Magnetic structures and alloys based on transition metal (TM) and rare-earth (RE) elements have been the focus of fascinating research due to the variety of peculiar properties characteristic of the combination of these two types of materials. The antiferromagnetic coupling between many RE and TM[1] can give rise to negative magnetoresistance (MR) both in multilayers[2] and alloys.[3,4] Recently, RE and their alloys have shown to affect drastically important magnetic properties in a TM layer, like polarization,[5] precessional frequency of the magnetization,[6] and damping.[7] Also, they have been used to reduce spin transfer noise in reading heads,[8] which could eventually be one of the main problems associated to their drastic reduction in size.[9]

Within RE, Gadolinium is of special interest because it is ferromagnetic up to room temperature ($T_C^{Gd} = 293$ K) and it has a very large magnetic moment at low temperatures. Permalloy doped with Gd has shown great potential for several applications, such as tuning the resonance frequency of a magnetic domain wall,[10] its velocity in magnetic nanostripes,[11] or even control the spin polarization of the material.[5,11]

In this work we study the influence of Gadolinium on the spin transfer torque (STT) using Permalloy (Py) based nanopillars. We report a remarkable increase in the critical current required to destabilize the Py layer when a Fe/Gd/Fe ferrimagnetic trilayer is added onto the structure. The origin of this enhanced stability cannot be understood solely with the macrospin approximation and we show that it is likely caused by a torque at the Fe/Gd interface that opposes the standard STT in the free Py layer. Our results are potentially very relevant for systems where the STT noise is an issue, like on hard drive reading heads where an increase of the critical current might be desirable. Indeed, other ferrimagnetic structures have been already successfully applied in spin valves in order to increase the critical current for STT.[12] The use of a thin layer of Gd seems to add stability to this type of structures with no or little detriment in their performance.

The basic structure used in this study is SiO2// Cu(60)/ CoFe(12)/ Cu(10)/ Py(4)/$\overline{\text{AFL}}$/Cu(8) where Py stands for permalloy ($Ni_{80}Fe_{20}$) and $\overline{\text{AFL}}$ is an artificial ferrimagnetic layer of Fe(1)/Gd(1)/Fe(1). The numbers represent the thickness in nanometers. The reason for using Fe/Gd/Fe rather than a single layer of Gd is that Gd diffuses in Co and Ni, but it forms a very sharp antiferromagnetic interface with Fe.[13,14] In addition, due to the exchange interaction at the interface with Fe, a thin Gd layer can remain ferromagnetic up to high temperatures (~1000 K),[14,15] which is very useful for room temperature or higher temperature operation.

In order to understand the effect of the AFL, we have also measured a control sample with only Py in the free layer (i.e., SiO2// Cu(60)/ CoFe(12)/ Cu(10)/ Py(4)/ Cu(8)). All samples were deposited by DC magnetron sputtering at room temperature on thermally oxidized Si substrates. The base pressure was always lower than 6×10^{-8} mbar. Special precautions were taken to avoid Gd oxidation and interface contamination, using only ultra-purified Ar and depositing the Gd and surrounding layers within few seconds. Scanning Transmission Electron Microscopy (STEM) combined with Electron Energy Loss Spectroscopy (EELS) was previously performed on these structures to check the continuity of the thin layers and the interfacial roughness.[14]

Using a combination of electron beam lithography and ion milling, the films were then patterned into elliptical pillars of 50 by 150 nm (cross sectional area $S = 5.9 \times 10^{-3}\ \mu m^2$). The pillars were partially patterned to the intermediate Cu layer so the nanopillar corresponds only to the free layer. With this geometry, the bottom unpatterned CoFe layer is not affected by STT, which helps with the interpretation of the results. For both structures, we have measured a minimum of five devices both at RT and low T, obtaining a high consistency and good reproducibility of the results. The electrical measurements were performed with a DC current on a two contact geometry. We define positive current when the electrons flow from the reference unpatterned layer to the

free layer. Therefore, positive current favors stabilization of the parallel state (P) while negative current favors the antiparallel state (AP).

Figure 1(a) shows a typical R-H loop for both devices. As it can be seen, in both samples, after saturation, the free layers switches before reaching $H=0$. This is due to strong dipolar field acting on the free layer, likely caused by a small over-milling that reached the reference CoFe layer. By measuring minor loops on our samples, we can directly extract the coercive field in both samples H_C^{free} (see Figure 1(a)) and then the dipolar field can be easily obtained from the R-H curve at I = 0. The value of this dipolar field is approximately $H_d \sim 70$ Oe for the AFL device and 55 Oe for the Py device. The coercivity of the CoFe unpatterned layer is $H_C^{CoFe} = 32$ Oe for both samples and the coercivity of the free layer is around $H_C^{free} = 60$ Oe for the AFL devices and 55 Oe for the Py device once patterned. Interestingly, for the Py/AFL device, the dipolar field induces a double transition of the free layer as shown by the dotted line in Fig. 1(a). Coming from positive saturating field, the free layer switches first at around +20 Oe, then at −32 Oe the CoFe layer reverses, forcing the free layer to switch again due to the dipolar field, going back to having both layers antiparallel. This antiparallel arrangement is sustained until the external field reaches $H_d + H_C^{free} \sim 135$ Oe. For zero current, this double switching is only found in the Py/AFL samples and it is very obvious in some other devices (not shown here). The reason is the higher dipolar field in the AFL samples and the higher magnetic moment of the Py/AFL layer, which is therefore more affected by the dipolar field.

Let us first analyze the results at low temperature, measured on a cryostat at 10 K. Fig. 1(b) shows the *R-I* loop at a small magnetic field for both samples following the sequence $I=0 \rightarrow -I_{max} \rightarrow +I_{max} \rightarrow I=0$. Both devices begin in the P state (minimum resistance) and switch to the AP state at a given negative critical current $I_C^{P\rightarrow AP}$ which is considerably higher for the device with AFL. The AP state remains stable until $-I_{max}$. By applying positive current, the control sample switches back to the P state at a critical current $I_C^{AP\rightarrow P}$ as expected from the STT (Fig. 1(b) top). In this control device $|I_C^{P\rightarrow AP}| > |I_C^{AP\rightarrow P}|$, which is the usual behavior in the Slonczewski model.[16] On the other hand, the maximum positive current applied in our measurements is not large enough to switch the device with the AFL back to P state. This means that $I_C^{AP\rightarrow P} > 9.5$ mA for this device and $|I_C^{P\rightarrow AP}| < |I_C^{AP\rightarrow P}|$, in contrast to the usual behavior.

Figure 2 shows selected *R-I* loops measured at 10 K for the control sample and the corresponding phase diagram. The colored diagram has been obtained by plotting the positive branch (i.e., the branch that goes from $-I_{max}$ to $+I_{max}$) of the *R-I* loops for different fields. Between each *R-I* loop

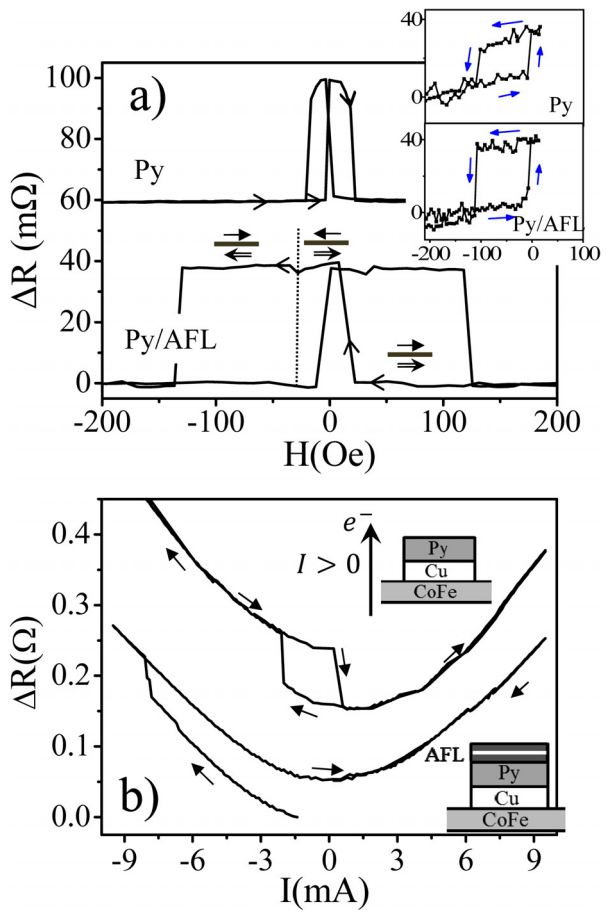

FIG. 1. (a) Room temperature R-H loops for the Py device top and the AFL device bottom. The loops are vertically displaced for clarity. In the bottom loop for the Py/AFL device, the dotted line indicates the switching field of the bottom CoFe layer. The cartoons with arrows indicate the direction of the CoFe (double arrow) and free layer (single arrow) at different fields on the negative branch of the loop. The insets show the minor loops of the free layers. (b) ΔR-I loops at 10 K and low field for a control sample with Py as free layer (top) and for the Py/AFL device (bottom). The loops are vertically displaced for clarity. The cartoons represent the structure of the Py and the Py/AFL devices.

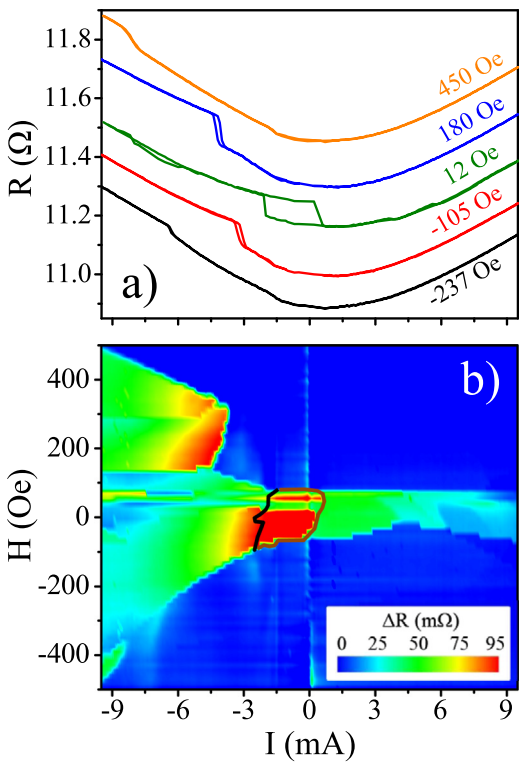

FIG. 2. Selected *R-I* loops at different fields at 10 K for a control Py device (a) and stability phase diagram (b). The current sequence was $I=0 \rightarrow -I_{max} \rightarrow +I_{max} \rightarrow 0$. The quadratic effect of the Joule heating depends on the direction of the current (smaller slope for negative currents). This is probably due to the Peltier effect in the structure.

the device was saturated in the negative direction to reset its magnetic state. ΔR was obtained by subtracting an *R-I* reference loop measured at saturation (stable P state) to the *R-I* curve for every field value. Therefore, $\Delta R = 0$ corresponds to P state (dark blue in the diagrams). In order to include in the diagram the information of the negative branch (from $+I_{max}$ to $-I_{max}$), we have added colored lines to highlight the different transitions. A brown line indicates a transition from AP to P-state in the positive branch ($-I_{max}$ to $+I_{max}$) and a black line represents transitions from P to AP-state on the negative branch of the *R-I* loop. Therefore, these two lines enclose the hysteretic bistable AP-P region of the diagram.

For this control sample with only Py in the free layer, the highest coercivity is obtained at 55 Oe, with $I_C^{P\to AP} = -2.1$ mA and $I_C^{AP\to P} = +0.6$ mA, resulting in a switching critical current of $\langle I_C\rangle = (I_C^{AP\to P} - I_C^{P\to AP})/2 = 1.35$ mA (2.3×10^7 A/cm^2). Note also that outside the hysteretic area, reversible transitions are predominant up to very high fields where the critical current increases linearly with the field, as expected from the Slonczewski model. This might be an indication of a sustained precession of the free layer at high fields, although this could not be confirmed in our measurements up to 6 GHz.

The phase diagram for the sample with the AFL is shown in Fig. 3(b). The red area that represents the hysteretic region is much broader in this sample. It is clear that once the Fe/Gd/Fe layer is added to the structure, both $I_C^{AP\to P}$ and $I_C^{P\to AP}$ experience a dramatic increase. In fact, the current cannot switch from AP to P-state in the hysteretic region (from -29 Oe to 70 Oe). This implies that $I_C^{AP\to P}$ is higher than 9.5 mA, the maximum current applied. For this sample,

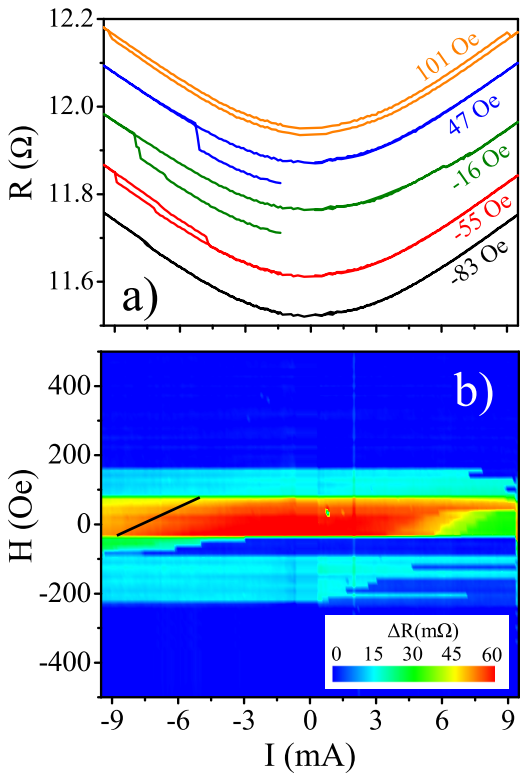

FIG. 3. Selected *R-I* loops at different fields at 10 K for a sample with AFL on the free layer (a) and corresponding stability phase diagram (b). The current sequence was again $I = 0\to -I_{max}\to +I_{max}\to 0$.

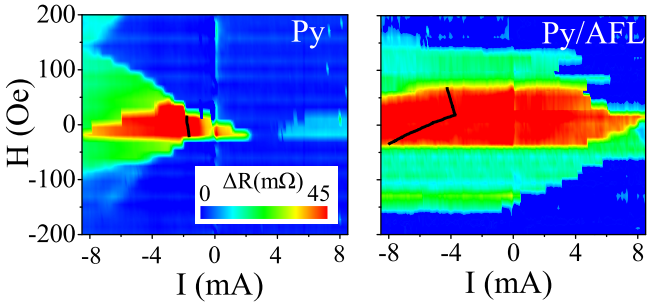

FIG. 4. Stability phase diagram at room temperature for a sample with Py as free layer (left) and Py/AFL (right), showing the increase on current stability by adding the AFL to the structure.

the highest coercivity is obtained at -29 Oe, with $I_C^{P\to AP} = -9$ mA and $I_C^{AP\to P}$ at least $+9.5$ mA. Therefore $\langle I_C\rangle = 9.25$ mA (1.6×10^8 A/cm^2), almost an order of magnitude higher than in the Py sample. The light blue areas of Fig. 3(b) show irreversible transitions from P to an intermediate state of small ΔR (see also red and orange loops in Fig. 3(a), which might be associated to metastable domain formation that can be removed by large positive currents, returning the device to P-state.

Before discussing the results, we show in Fig. 4 the phase diagrams for both a Py sample and an AFL sample at room temperature. As it can be seen, the AFL sample has still a much larger critical current. This was expected as a thin Gd layer remains ferromagnetic between the Fe layers, as shown by ourselves and other authors in previous reports.[14,15] At room temperature, the critical current in a Py sample is measured around 1.7 mA (2.9×10^7 A/cm^2), while for a sample with AFL the critical current is approximately 7.9 mA (1.3×10^8 A/cm^2), almost 5 times larger than in the control sample.

In order to understand the reasons behind the larger stability of the sample with AFL, we have studied the effect of the Fe/Gd/Fe trilayer on the magnetic properties of the Py layer. In Fig. 5 we show the Ferromagnetic Resonance measurements performed on unpatterned films with the same structure and thickness of the free layer in our devices. By fitting to the Kittel formula many pairs of values ($\Delta f - H_{EXT}$) in the high field region, and determining experimentally the M_S and the gyroscopic constant γ, our measurements lead to a damping factor of $\alpha_{Py} = 0.02$ for Py, which is quite high for this material, and $\alpha_{Py-AFL} = 0.011$ for a Py/AFL layer. These values, obtained in films at RT, may

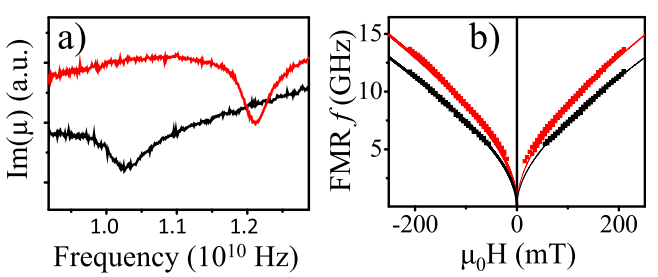

FIG. 5. (a) Imaginary part of the permeability measured at high fields and room temperature on a Py(4 nm)-film (black) and a Py(4 nm)/Fe(1 nm)/Gd(1 nm)/Fe(1 nm)-film (red). (b) Ferromagnetic resonance data (symbols) adjusted to the Kittel equation (line).

change on the patterned nanometric devices but they are a good indication for our discussion. We have measured also the values of M_S at RT, extracted from the hysteresis loops measured with the field applied perpendicular to plane for films with the same thickness as the ones used in the devices. The values obtained are $\mu_0 M_S = 0.55$ T for Py and 0.85 T for Py-AFL. Please note that the saturation magnetization of Py can be considerably smaller in thin films compared to the bulk value.[17] The value of M_S at 10 K for the films was also extracted using a SQUID magnetometer, resulting in $\mu_0 M_S(\text{Py}) = 0.7$ T and $\mu_0 M_S(\text{Py-AFL}) = 1$ T.

In the macrospin approximation, the critical current for spin transfer reversal is described by the following expression:

$$I_c = \frac{2e\alpha M_S St}{\hbar g(\theta) p} \times H_{eff},$$

where M_S, S, t, α, p, $g(\theta)$, and H_{eff} are the magnetization, surface, thickness, damping, polarization, angular factor, and effective field acting on the free layer, respectively. Ideally, the comparison between both samples should be done when the hysteretic region in the stability diagrams is centered on $H_{eff} = H_{app} + H_d = 0$. In our samples this is not possible though, as the coercivity of the CoFe bottom layer is smaller than the dipolar field and its switching occurs before H_{app} can compensate H_d. On the other hand, the stability phase diagrams show that the increase of I_C from a Py sample to an AFL sample is very similar in the entire hysteretic region (red area) so we can always compare I_C at a similar effective external field $H_{app} + H_{dip}$ in both devices.

From the macrospin approximation we can see that $I_c/(\alpha M_S St) \propto H_{eff}/p$. Introducing all the values measured at RT, we obtain $I_C/(\alpha M_S St) = 7.1 \times 10^8\,\text{Acm}^{-2}\,\text{nm}^{-1}\text{T}^{-1}$ for the control sample and $20 \times 10^8\,\text{Acm}^{-2}\,\text{nm}^{-1}\text{T}^{-1}$ for the AFL sample, a factor 3 increase which is only slightly smaller to our experimental findings. As we are comparing these amounts at similar H_{eff}, the increase of the critical current could be interpreted either by a reduction of the spin polarization by a factor of 3 due to the introduction of the AFL[18] or by the AFL providing somehow an additional way to dissipate energy and rate of work by the spin torque.[12] None of these two explanations is satisfactory due to the following reasons. First, the values of ΔR in both samples are quite similar, indicating that the spin polarization p is also quite similar in the two samples. Note that the thickness of the Py under the Fe/Gd/Fe trilayer is 4 nm, similar to the spin diffusion length of Py (5 nm) and it has been shown by ourselves and other authors that for this thickness of Py (or larger) the value of ΔR should not be affected by the presence of topping layers.[8,18,19] Second, if any of the above two explanations were correct, one would expect an increase of $|I_C^{P\to AP}|$ (electrons flowing from AFL to the CoFe layer), and similar or smaller increase of $|I_C^{AP\to P}|$. This is indeed what was observed when a Synthetic Antiferromagnetic layer was introduced in the free layer[12,20] or when a capping layer increases the damping α in the free layer,[8] but it is the opposite to our observations. In our case, it is $|I_C^{AP\to P}|$ the one that increases more dramatically by introducing the AFL. This suggests that an entire different mechanism is behind the enhanced stability introduced by the Fe/Gd/Fe trilayer.

In rare-earths both the conduction and binding are due to electrons which only have a small contribution to the magnetic moment of the substance and most of this moment comes from the strongly localized 4f electrons on the rare earth atoms. Therefore, in our AFL devices for positive currents, all the angular momentum carried by the spin polarized current in the Py layer must be transferred to the antiparallel Gd layer at the interface between the 3d Py/Fe and the 4f Gd. The effect of this sudden transfer of angular momentum can be observed experimentally in any standard Spin Valve just by inserting a very thin Gd layer between the non-magnetic layer and the free layer. By doing so, the MR value drops to zero[21] indicating that all the spin information is lost at the interface between the Gd and the transition metal. We have also done some calculations of spin accumulation and torque in the different layers (not shown here) and the profile in Gd changes only for a spin diffusion length below 0.5 nm, which agrees with our argument.

In the control Py device, the free layer suffers the standard STT that destabilizes the AP state for positive current at $I_C^{AP\to P}$. On the other hand, for the devices with the AFL, the free layer must experience an additional torque that comes from the sudden spin transfer at the antiferromagnetic Gd/Fe interface. As the Gd couples antiferromagnetically with the rest of the free layer, this additional torque goes in the opposite direction to the standard one and would promote the AP configuration of the entire free layer for positive current, leading to an effective increase of the critical current $I_C^{AP\to P}$.

The opposite contribution to the torque caused by the antiparallel Gd should be stronger in the positive current direction, when the electrons flow from the reference layer towards the Py/AFL free layer. For negative current direction, only electrons reflected at the CoFe layer destabilize the free layer magnetization. This is in good agreement with our experimental results, where we observe that the increase of the critical current from the Py control devices to the AFL devices, is higher for the positive current direction, even resulting on $|I_C^{AP\to P}| > |I_C^{P\to AP}|$, which is opposite to what is usually measured.

The Fe layer by itself cannot be the cause of the enhancement of the critical current. Its spin polarization has a similar value of that of Co, Ni, or Py and, more significantly, the same sign.[22–24] Therefore, the Py/Fe ferromagnetic boundary is unlikely going to contribute to an opposite torque like the Fe/Gd antiferromagnetic interface.

In conclusion, we have shown that a thin trilayer of Fe/Gd/Fe can stabilize the free layer of Py-based nanopillars against STT. At 10 K, the factor of enhancement can be almost an order of magnitude, while at RT it can increase by a factor of 5. By measuring the values of Gilbert damping and saturation magnetization of the free layer, we show that this effect cannot be explained solely by the Slonczewski macrospin model. We argue that this enhancement of the critical current in the sample with AFL is due to an additional torque at the Fe/Gd interface that goes in the opposite direction to the main spin transfer torque. The total ΔR of the device does not change much by adding Fe/Gd/Fe, as the thickness of the Py layer underneath is of the order of its spin diffusion length. Therefore, this type of trilayers might

constitute a potential solution to problems of stability in some nanometer-size devices.

This work was funded by MAT2011-28532-C03-03 and MAT2009-08771 from the Spanish Ministerio de Ciencia e Innovación. M.R. was supported by a FPU fellowship AP2007-00464.

[1]R. E. Camley and R. L. Stamps, J. Phys.: Condens. Matter **5**, 3727 (1993).
[2]F. E. Stanlet, M. Perez, C. H. Marrows, S. Landridge, and B. J. Hickey, Europhys. Lett. **49**, 528 (2000).
[3]D. Z. Yang, B. You, X. X. Zhang, T. R. Gao, S. M. Zhou, and J. Du, Phys. Rev. B **74**, 024411 (2006).
[4]C. Bellouard, H. D. Rapp, B. George, S. Mangin, G. Marchal, and J. C. Ousset, Phys. Rev. B **53**, 5082 (1996).
[5]C. Kaiser, A. F. Panchula, and S. S. P. Parkin, Phys. Rev. Lett. **95**, 047202 (2005).
[6]S. G. Reidy, L. Cheng, and W. E. Bailey, Appl. Phys. Lett. **82**, 1254 (2003).
[7]G. Woltersdorf, M. Kiessling, G. Meyer, J. U. Thiele, and C. H. Back, Phys. Rev. Lett. **102**, 257602 (2009).
[8]S. Maat, N. Smith, M. J. Carey, and J. R. Childress, Appl. Phys. Lett. **93**, 103506 (2008).
[9]J. G. Zhu and X. Zhu, IEEE Trans. Magn. **40**, 182 (2004).
[10]S. Lepadatu, J. S. Claydon, D. Ciudad, C. J. Kinane, S. Langridge, S. S. Dhesi, and C. H. Marrows, Appl. Phys. Lett. **97**, 072507 (2010).
[11]R. L. Thomas, M. Zhu, C. L. Dennis, V. Misra and R. D. McMichael, J. Appl. Phys. **110**, 033902 (2011).
[12]N. Smith, S. Maat, M. J. Carey, and J. R. Childress, Phys. Rev. Lett. **101**, 247205 (2008).
[13]J. Landes, Ch. Sauer, B. Kabius, and W. Zinn, Phys. Rev. B **44**, 8342 (1991).
[14]M. Romera, M. Muñoz, M. Maicas, J. M. Michalik, J. M. de Teresa, C. Magén, and J. L. Prieto, Phys. Rev. B **84**, 094456 (2011).
[15]D. Haskel, G. Srajer, J. C. Lang, J. Pollmann, C. S. Nelson, J. S. Jiang, and S. D. Bader, Phys. Rev. Lett. **87**, 207201 (2001).
[16]J. C. Slonczewski, J. Magn. Magn. Mater. **159**, L1 (1996).
[17]J. P. Nibarger, R. Lopusnik, Z. Celinski, and T. J. Silva, Appl. Phys. Lett. **83**, 93 (2003).
[18]N. C. Emley, F. J. Albert, E. M. Ryan, I. N. Krivorotov, D. C. Ralph, R. A. Buhrman, J. M. Daughton, and A. Jander, Appl. Phys. Lett. **84**, 4257 (2004).
[19]D. Lacour, J. A. Katine, N. Smith, M. J. Carey, and J. R. Childress, Appl. Phys. Lett. **85**, 4681 (2004).
[20]M. J. Carey, N. Smith, S. Maat, and J. R. Childress, Appl. Phys. Lett. **93**, 102509 (2008).
[21]M. Romera, M. Muñoz, P. Sánchez, C. Aroca, and J. L. Prieto, J. Appl. Phys. **106**, 023922 (2009).
[22]R. J. Soulen, Jr., J. M. Byers, M. S. Osofsky, B. Nadgorny, T. Ambrose, S. F. Cheng, P. R. Broussard, C. T. Tanaka, J. Nowak, J. S. Moodera, A. Barry, and J. M. D. Coey, Science **282**, 85 (1998).
[23]A. Berthélémy, A. Fert, and F. Petroff, *Handbook of Ferromagnetic Materials* (North Holland, Amsterdam, 1999), Vol. 12, p. 1.
[24]J. M. D. Coey, *Spin Electronics*, edited by. M. Ziese and M. J. Thornton (Berlin: Springer, 2001), Chap. 12, p. 279.